

# SPATIAL GRADIENTS IN AEROSOL OPTICAL DEPTH AND COLUMNAR SIZE CHARACTERISTICS OVER ARABIAN SEA AND TROPICAL INDIAN OCEAN

Auromeet Saha<sup>1</sup> and K Krishna Moorthy<sup>2</sup>

<sup>1</sup>Aryabhata Research Institute of Observational Sciences, Manora Peak, Nainital-263129, India

<sup>2</sup>Space Physics Laboratory, Vikram Sarabhai Space Centre, Trivandrum-695022, India.

## INTRODUCTION

During the periods when winds are calm over the oceans, so that local sea-salt production is quite low, and the advection of continental aerosols by prevailing circulations persists (like during the northeasterly winds over south Asia during winter), there will exist a gradient in aerosol concentration and optical depth from the landmass over to the ocean. This gradient would be a function of the loading over the land and the prevailing wind speed and direction. Estimates of gradients in aerosol optical depth, mass loading, and size characteristics over oceanic regions are useful in assessing the impact of aerosols from the continents in influencing the aerosol characteristics over the remote oceans and also in understanding the role of synoptic scale transport of continental aerosols over to oceans. Estimation of such gradients was also one of the important objectives of INDOEX (Ramanathan *et al.*, 1996). In this paper, we present results on the spatial gradients of aerosol optical depth and retrieved columnar size characteristics over Arabian Sea and tropical Indian Ocean.

## EXPERIMENTAL DETAILS AND DATA

The experimental data consisted of spectral aerosol optical depth (AOD) and retrieved columnar size characteristics estimated using a 10-channel Multi-Wavelength solar Radiometer (MWR) and 4-channel Eko Sun Photometer (ESP) as a part of Indian Ocean Experiment (INDOEX) cruise campaigns in 1998 and 1999 on board R/V Sagar Kanya. The instrumental details, data analysis, and cruise tracks are given in Moorthy *et al.* (2001) and Saha and Moorthy (2004).

## RESULTS AND DISCUSSION

### Gradients in Aerosol Optical Depth

For estimating the gradients in the AODs, their variations were examined as a function of the distance  $D$  (in km) from the Indian coast to the various oceanic locations where the observations are made, along the mean down-wind direction. For locations very near to the coast,  $D$  was taken as the normal distance from the observation point to the coast. This is because very close to the coast, the land/sea breeze circulations modify the prevailing winds within the boundary layer, where the aerosol abundances are large. For farther locations, the distance is estimated along the mean wind direction, from the



Indian coast to the point of observation. Here, it is to be noted that, advection of aerosols from land is not restricted to the mean winds and surface streamlines, but organized air trajectories also contribute significantly. However, this is not considered in this study. This is a simplified approach and the deduced estimates of the gradients can be somewhat over-estimated. Nevertheless, this approach provides a first order estimate of the nature of the gradients that can readily be parameterised using simple functions and are useful for impact assessment. Further, this approach also assumes implicitly that the spatial distribution of aerosol characteristics remains temporally stable over the vast area considered, so that the AOD estimated over various oceanic locations can be considered as a snapshot of a temporally stable population.

Following the above considerations, the AODs estimated at each of the oceanic locations are plotted (in logarithmic scale) against the distance  $D$  and are shown in Fig.1a for JFP-98, and Fig.1b for JFP-99 for the MWR (left panel) and ESP data (right panel) respectively. The individual points correspond to the measured AOD ( $\tau_p$ ) values and the straight line is the linear least square fit of the observation points to the equation,

$$\tau_p = \tau_{pc} \exp\left(-\frac{D}{D_o}\right) \quad \dots (1)$$

where  $\tau_{pc}$  is the coastal AOD (which is given by the Y-intercept), and  $D_o$  the distance at which the AOD falls to  $e^{-1}$  of its value at the coast. Notwithstanding a fair amount of scatter at some wavelengths, the points, in general, agreed with Eq.(1) at all the wavelengths, with the correlation coefficients ( $\gamma_c$ ) for different wavelengths lying in the range 0.26 to 0.87, and were significant at  $P = 0.02$  (98%) level (Fisher, 1970). The correlation coefficients are higher at shorter wavelengths, and lower at longer wavelengths, showing that the AODs at shorter wavelengths that are ascribed to sub-micron aerosols, comply better with Eq.(1). Using Eq.(1), a scaling distance  $D_{1/2}$  is estimated at each wavelength, as the distance at which the AOD falls to half of its value ( $\tau_{pc}$ ) at the coast.  $D_{1/2}$  is a measure of the gradients in AOD and is used to characterise the distance over the ocean, up to which the continental effects are felt significantly, as far as the aerosols are concerned. The values of  $D_{1/2}$ , thus estimated, ranged from 1000 to 3000 km at various wavelengths, with a mean value (considering all the wavelengths of MWR and ESP) of  $1718 \pm 537$  km for 1998 and  $1648 \pm 570$  km for the 1999 cruise, which are well comparable. The values of  $D_{1/2}$  remained quite similar in 1998 and 1999, thereby indicating that, the average north-south gradient in AOD is nearly the same during both the years.



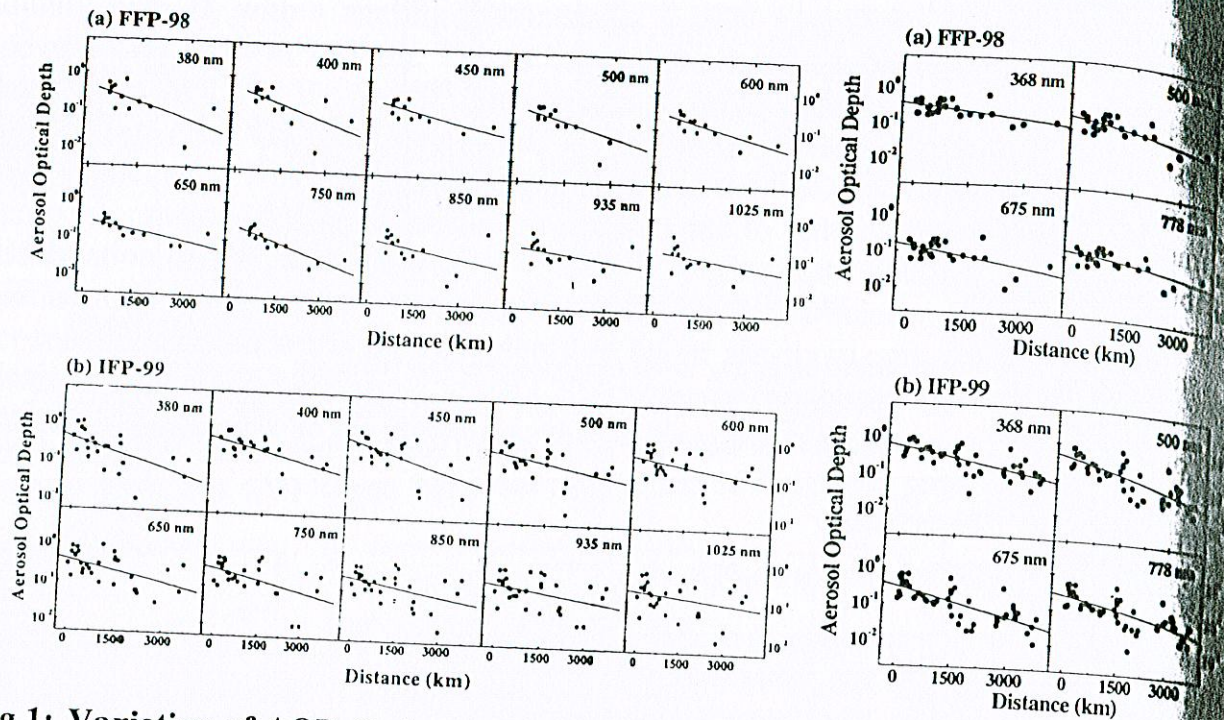


Fig.1: Variation of AOD (in logarithmic scale) with distance  $D$  from the Indian coast along the mean downwind direction for (a) FFP-98 (top panel) and (b) IFP-99 (bottom panel). The 10 frames in the left are for the MWR data and the 4 frames in the right are for the ESP data.

#### Wavelength Dependence of $D_{1/2}$

The variation of  $D_{1/2}$  with wavelength is shown in Fig.2a, separately for 1998 and 1999. It can be seen from the figure that  $D_{1/2}$  increases with increase in wavelength, gradually and then more rapidly.  $D_{1/2}$  is  $\sim 1000$  to  $2000$  km at shorter (visible) wavelengths ( $\lambda < 750$  nm), and increases to  $\sim 2500$  to  $3000$  km at the longer (near IR) wavelengths. In other words, the gradient is steeper at shorter wavelengths and shallow at longer wavelengths. The shallow gradient at longer wavelength is consistent with the weak spatial variation of AOD. Further, it is also seen that the nature of the wavelength dependence of  $D_{1/2}$  is broadly similar in both the years.



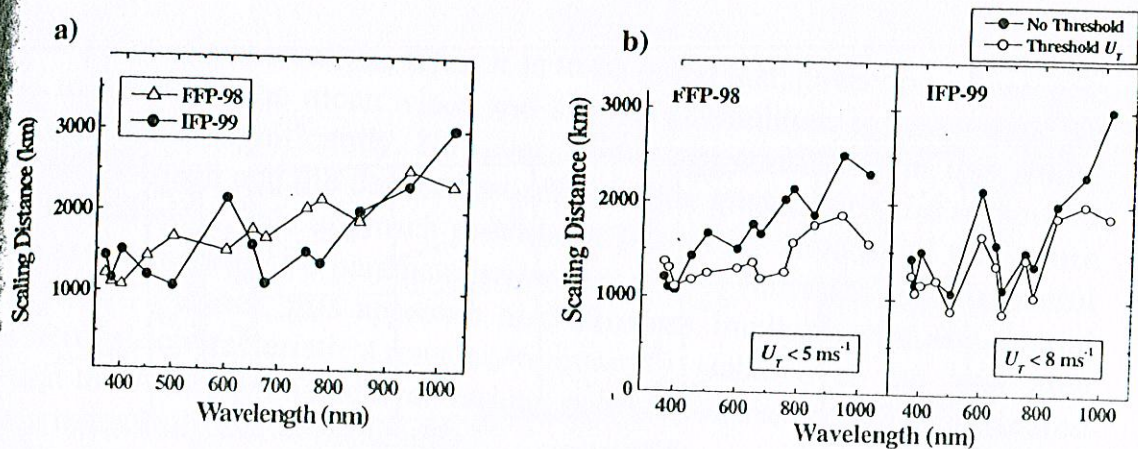


Figure 2: (a) Variation of  $D_{1/2}$  with wavelength for FFP-98 and IFP-99. (b) Variation of  $D_{1/2}$  with wavelength for FFP-98 (left panel) and IFP-99 (right panel) for two cases, one without threshold for wind speed (filled circles) and the other with threshold (open circles). The thresholds for wind speed ( $U_T$ ) are given at the bottom of each frame.

### Wind speed Dependence of $D_{1/2}$

With a view to examine the effect of wind speed in modifying the gradients, the AOD data sets for both the years have been divided into two groups and analysed separately following Eq.(1). The first group consisted of the entire data obtained under all wind speed conditions, and the other group consisted of only those data, when the mean wind speed was less than a threshold value. The threshold value was chosen as  $5 \text{ m s}^{-1}$  for FFP-98, and  $8 \text{ m s}^{-1}$  for IFP-99. Different thresholds were considered for the two cruises mainly because, the wind speeds encountered in FFP-98 were generally lower, and showed a median value of  $5 \text{ ms}^{-1}$ ; whereas during the IFP-99 cruise, the median value was found to be  $\sim 8 \text{ ms}^{-1}$ . With AODs separated as above, the scaling distance  $D_{1/2}$  was estimated at all the wavelengths, separately for FFP-98 and IFP-99 following the least square fit to Eq.(1). The variations of  $D_{1/2}$  as a function of wavelength are shown for these cases in Fig.2b, with the left panel for 1998 and the right panel for 1999. The increase in  $D_{1/2}$  at longer wavelengths ( $\lambda > 750 \text{ nm}$ ) is seen in both the cases, when the entire data irrespective of wind speed are considered. But when the high wind (i.e., wind speed greater than threshold) values are removed, the tendency of  $D_{1/2}$  to increase with wavelength is considerably reduced. This confirms the effect of strong winds in reducing the spatial gradients (increasing the scaling distance), particularly at the longer wavelengths by selective enhancement of large/super-micron aerosols produced by sea-spray activity.

### Gradients in Retrieved Parameters

The physical parameters of aerosols such as  $M_L$ ,  $R_{eff}$ ,  $r_{m1}$ ,  $r_{m2}$ ,  $\sigma_{m1}$ ,  $\sigma_{m2}$ ,  $N_a$ ,  $N_c$  estimated from the columnar size distributions for each observation day are examined (Saha and Moorthy, 2004). In the light of the broad similarity in AOD spectral dependence as well as the nature of the variations of other retrieved parameters in 1998



and 1999 cruises, these two data sets are considered together as a single set. Fig.3a shows the variation of  $R_{eff}$  (top panel), and  $M_L$  (bottom panel) with distance  $D$ .  $M_L$  decreases gradually with  $D$ , with a scaling distance  $D_{1/2} \sim 1900$  km, which is comparable to the value of  $D_{1/2}$  for AOD at 750 nm. This is because the coarse, super micron aerosols (which influence the AODs at the longer wavelengths) are the chief contributors to the aerosol mass loading also. On the other hand,  $R_{eff}$  shows a positive gradient, increasing with increase in distance. This is due to the rapid change in the CSD caused by the faster decrease in the concentration of fine/accumulation aerosols due to reduced source impacts and size transformation due to microphysical processes and rather slow decrease of coarse particle concentration. These changes occur more rapidly at the sub-micron sizes, whereas at the super-micron sizes the loss is partly replenished by the sea-spray particles. Thus, the relative abundance of sub-micron aerosols in the CSD decreases considerably at far away locations.  $R_{eff}$  increases in response to the above decrease in  $N_a$ .

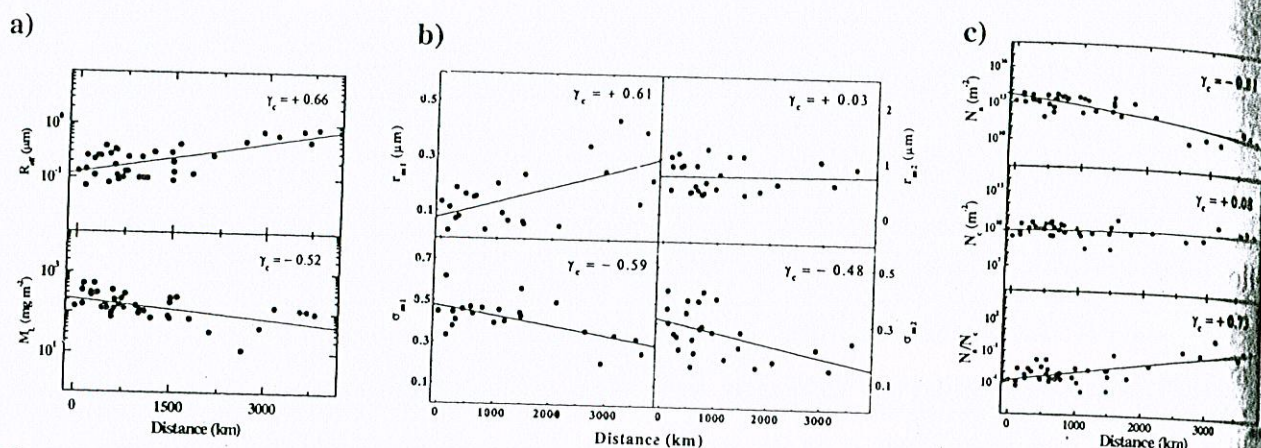


**Figure 3:** (a) Variation of  $M_L$  (bottom), and  $R_{eff}$  (top) with distance  $D$ . (b) Variation of  $r_{m1}$ ,  $\sigma_{m1}$ ,  $r_{m2}$ , and  $\sigma_{m2}$  with distance (c) Variation of  $N_a$  (top panel),  $N_c$  (middle panel), and  $N_c/N_a$  (bottom panel) with distance. The points are the individual observations, and lines are the least square fit.

The variations of the  $r_{m1}$ ,  $r_{m2}$ ,  $\sigma_{m1}$  and  $\sigma_{m2}$  are shown in Fig.3b.  $r_{m1}$  shows a general increasing trend with  $D$ . Closely associated with the growth in the fine aerosol mode, there is a steady decrease in its width, as can be seen from the decrease of  $\sigma_{m1}$  with  $D$ . On the other hand, the coarse mode does not show any significant changes in  $r_{m2}$  and  $\sigma_{m2}$  shows only a weak decreasing trend. The variation of  $N_a$ ,  $N_c$  and  $N_c/N_a$  (a measure of the relative abundance of accumulation mode aerosols over the coarse ones) with distance are shown in Fig.3c. There is a rapid decrease in  $N_a$  with distance. This sharp decrease in  $N_a$  can be a major factor responsible for the increase in  $R_{eff}$ . However,  $N_c$  does not show any significant variation with distance. The variation of the  $N_c/N_a$  (bottom panel of Fig.3c) shows that, there is a net increase in the relative abundance of coarse particles as we move to open Ocean. This is due to the relative dominance of smaller particles (accumulation mode) as one approach the coast, which can be attributed to the anthropogenic activities over the continent.



## CONCLUSIONS

1. The AODs gradually decreased with increase in distance from the Indian coast, with  $D_{1/2}$  in the range ~1000 to 3000 km at different wavelengths and different years.
2. The gradients in AODs showed wavelength dependence, being steeper at shorter wavelengths and shallower at longer wavelengths ( $\lambda > 750$  nm).
3. The gradients in AODs also showed wind speed dependence, being steeper at low wind speeds and shallower with increase in wind speeds, and this effect was found to be more significant at longer wavelengths.
4. The columnar mass loading decreased with increase in distance from the coast, with a scaling distance  $D_{1/2}$  ~1900 km. However, the effective radius and the primary mode radius showed an increasing trend with distance, which was attributed mainly to the microphysical processes.
5. The number concentration of accumulation mode aerosols decreased rapidly with increase in distance from the coast. The secondary mode radius and the concentration of coarse aerosols didn't show any significant variation with distance, thereby indicating that these particles are mainly of marine origin and hence do not undergo significant variations over the oceanic regions.

## REFERENCES

- Fisher, R.A. (1970) Statistical methods for research workers, Oliver and Boyd, Edinburgh.
- Moorthy, K.K., *et al.* (2001) *J. Geophys. Res.*, **106**, 28539-28554.
- Ramanathan, V., *et al.* (1996) A multi-agency proposal for a field experiment in the Indian Ocean, C4 publication #162, Scripps Institute of Oceanography, La Jolla.
- Saha, A., and K.K. Moorthy (2004) this issue of *IASTA Bulletin*..